International Journal on Engineering Technology (InJET)

www.kec.edu.np/kec-journal/
Volume 2, issue no. 1, Dec 2024, Page 19-28
Received Date: Aug 15, 2024
Accepted Date: Oct 6, 2024
ISSN: 3021-940X (Print)
DOI: https://doi.org/10.3126/injet.v2i1.72487

Precise Excitation of a Switched Reluctance Machine under Regenerative Mode in High-Speed Operation

Slamet Riyadi[1,*], Leonardus Heru Pratomo[2]

[1]*Dept. of Electrical Engineering – Soegijapranata Catholic University, Pawiyatan Luhur IV-1, Semarang - Indonesia, riyadi@unika.ac.id ,*

[2]*Dept. of Electrical Engineering – Soegijapranata Catholic University, Pawiyatan Luhur IV-1, Semarang - Indonesia, leonardus@unika.ac.id*

Abstract

The implementation of electric machines in electric and hybrid electric vehicles offers some advantages, including the ability to operate in regenerative mode. Switched reluctance (SR) machines have been alternative solutions due to their characteristics. Operating an SR machine in propulsion mode requires high torque and minimal torque ripple, while producing optimal output power in regenerative mode is required. In high-speed operation, when the back electromotive force is greater than the DC link voltage, single pulse-based methods are often used. Torque ripple problems can be neglected due to rotor inertia. In this paper, a single pulse-based control for SR machines in high-speed operation under regenerative and discontinuous conduction modes is analyzed. Excitation to magnetize the rotor and generation process to produce output power are compared to determine the effectiveness of energy saving during regenerative mode. By using a simple control strategy, precise excitation angles can be obtained to turn the machine on and off. Experimental work has been done to support the analysis. They show that by using proper excitation angles, the optimal output power can be generated.

Keywords: switched reluctance machine, regenerative mode, single pulse excitation, back EMF, inductance profile

1. Introduction

Switched reluctance (SR) machines have been alternative solutions for electric drives because they offer some advantages due to simple construction, low manufacturing cost and brushless operation. Switched reluctance machines can also operate under motoring and regenerative modes, which is very important for electric vehicles (EV) and hybrid electric vehicles (HEV) (Cheng, et.al., 2020), (Tiwari & Saxena, 2019), (Sun, et.al., 2019), (Aiso & Akatsu, 2020). Under motoring mode, high torque production with reduced torque ripple is very important, some control strategies have been developed to achieve these features in SR motors. They include direct and indirect control concepts. The first category can be implemented by directly controlling the torque by keeping the flux vector of the stator linkage at a nearly constant magnitude. Then, the motor torque is controlled by accelerating and decelerating the stator linkage flux vector (Ai-de, et.al., 2016), (Ai-de, et.al., 2018), (Yan, et.al., 2019). It is common to control the torque of the motor by converting torque references to phase current references. Since the torque in SR motors depends on the rotor position, the conversion of torque into current is not straightforward, such concepts are referred to as indirect torque control methods. Among these methods, the torque sharing function is the simplest and most powerful method. The torque ripple in the SR motor is mainly generated during the commutation period when the currents of multiple phases are in conduction. To achieve a nearly constant torque, each phase current must be coordinated to generate phase current references. Then the current controller will force the actual phase currents to follow these references (Peng, et.al., 2018), (Li, et.al., 2019), (Wei, et.al., 2106), (Kurian & Nisha, 2015).

In EV and HEV applications, the main energy recovery system during the regenerative mode depends on an electric machine operating as a generator. The ability to convert mechanical energy into electrical energy is limited by the parameters of the electric machine and the batteries (Arifin, et.al., 2012). Operation of an SR machine as a generator requires excitation during the negative slope of the phase stator inductance. Regulation of phase currents in this mode can be realized by using current controller or changing excitation angle in single pulse based control (Wahyu & Riyadi, 2019), (Zhu, et.al., 2020). The implementation of single pulse based control must also consider the limit of stable operation (Oprasic, et.al., 2013). To reduce the torque ripple of an SR machine, the current controller can be applied (Wang, et.al., 2017), (Sikder, et.al., 2014). The current controller can be based on the outgoing phase current, which depends on the incoming phase (Bogusz, 2017). Meanwhile, the use of single pulse based control still results in high torque ripple due to the current variation and double salient pole structure. By adding freewheeling operation in the generation process with single pulse based control, the torque ripple can be minimized although the generated output power is constant (Ling, et.al., 2017). High speed torque ripple can be suppressed by the inertia of the rotor and load. In high speed operation, current does not normally flow continuously through the phase stator winding, which means that the machine is operated in discontinuous conduction mode (DCM) under single pulse based control. In order to obtain optimum output power, the turn-on and turn-off angles must be precisely selected according to the rotor position. However, above a certain rotor speed, the excitation angles cannot be changed and the machine is operated in continuous conduction mode (CCM). In such a condition, the flux associated with the stator winding never drops to zero (Vujicic & Calasan, 2016), (Fernando, 2014). To improve the efficiency of an SR generator, the machine parameters can be used but this required complexity in calculations (Zine, et.al., 2023)

In this paper, a control strategy of an SR machine based on single pulse under discontinuous conduction of phase current is analyzed. Phase currents related to output power under excitation with different turn-on angle and fixed turn-off angle are studied to obtain precise excitation. To verify the analysis, experimental works with 16-bit microcontroller dsPIC30F to generate excitation angle were used. The angles are processed using the input capture facility available on the microcontroller.

2. Research Methods

2.1. Switched Reluctance Generator

Due to Faraday's law of induction, voltage can be induced across the terminals of coils under any change in magnetic field. Since an SR machine has neither permanent magnets nor windings on its rotor, the rotor must be magnetized by the stator windings for a certain period of time. Then, the moving rotor will induce back electromotive force (BEMF) on the stator windings. Figure 1 shows an SR machine with a 12-pole stator and an 8-pole rotor. A converter is required to operate an SR machine, Fig.2 shows an equivalent circuit of the SR machine connected to a DC source via a three-phase asymmetrical converter. Using one leg of such a converter, some equations can be derived based on these figures.

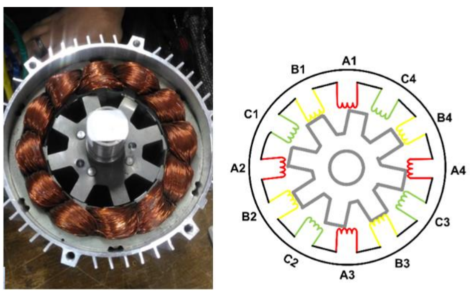

Figure 1. stator and rotor of a 12/8 SR machine

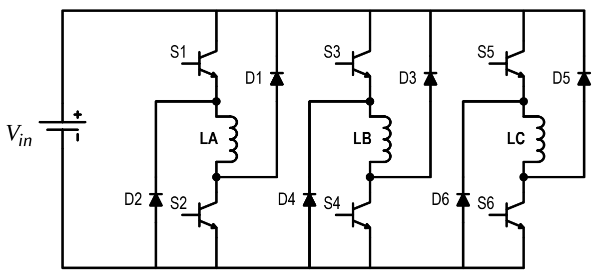

Figure 2. Equivalent circuit of an SR machine

$$V_{in} = R.i_{ph} + \frac{d\lambda(\theta, i_{ph})}{dt}$$ (Equation 1)

where,

V_{in} = input voltage

R = stator resistance
I_{ph} = stator phase current
λ = linkage flux
θ = angle of rotor position

For the linkage flux can be replaced by the multiplication of inductance and current, so we have

$$\lambda(\theta, i_{ph}) = L(\theta, i_{ph}).i_{ph} \qquad \text{(Equation 2)}$$

where,
L = stator inductance

Finally, Eq(1) can be stated as

$$V_{in} = R.i_{ph} + L(\theta, i_{ph})\frac{di_{ph}}{dt} + i_{ph}\omega\frac{dL(\theta, i_{ph})}{d\theta} \qquad \text{(Equation 3)}$$

where,
ω = rotor speed

The third term in the right-hand side of equation (3) is the back electromotive force (BEMF = e_b), whose magnitude is determined by the phase current, the rotor speed, and the slope of the phase inductance.

$$e_b = BEMF = i_{ph}\omega\frac{dL(\theta, i_{ph})}{d\theta} \qquad \text{(Equation 4)}$$

where,
e_b = back electromotive force (BEMF)

An asymmetrical converter always excites the SRM stator winding with unipolar currents, so the polarity of the BEMF is determined only by the gradient of the phase inductance. When the gradient of the phase inductance is positive, the BEMF has a positive polarity. Based on Eq.(3), the phase current will decrease, indicating that the energy conversion process from electrical energy to mechanical energy is taking place (motoring mode). Meanwhile, when the gradient of the phase inductance is negative, the BEMF has negative polarity. The phase current will increase, indicating that the energy conversion process from mechanical to electrical energy is in progress. It means that the SR machine is working in the generating mode.

The excitation of the stator winding of the SR machine in generating mode is shown in Fig.3. Usually, just before the aligned position between rotor and stator, switches S_1 and S_2 are turned on at θ_{on} to excite the stator winding, then the stator current will increase and its associated flux will increase. At θ_{off}, switches S_1 and S_2 are turned off and the current from the stator winding is sent back to the DC bus until the stator current tends to zero at θ_x (Fig.4). The interval between $\theta_{on}<\theta<\theta_{off}$ is called the excitation process, where the current from the DC link flows into the stator winding, while the generation process takes place during $\theta_{off}<\theta<\theta_x$, where the stator current flows back to the DC link through two diodes. In this process, the induced voltage in the stator winding is equal to the BEMF as expressed in equation (4).

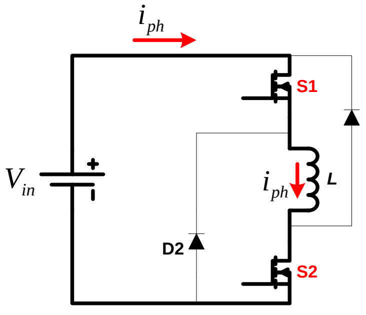

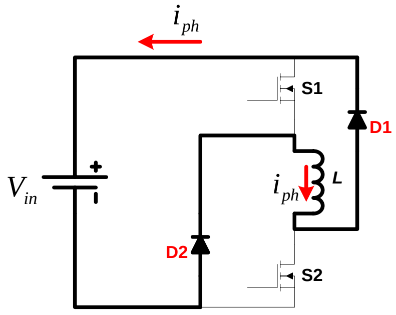

Figure 3. Equivalent circuit of one phase for SR machine under excitation process

Figure 4. Equivalent circuit of one phase for SR machine under generating process

The magnitude of the BEMF varies with the rotor speed and the behavior of the phase current, which depends on the relationship between the magnitude of the BEMF and the DC link voltage. Profiles of the phase current generated during the generation process are shown in Fig.6. When the BEMF is larger than the DC link voltage, the phase current continues to increase until θ_{u2} (the angle at which the minimum inductance of the stator winding is reached) after the switches are turned off, and then decreases to zero. Such a condition is found in high-speed operation. When the BEMF is equal to the DC link voltage, the phase current will be nearly constant after two switches are turned off up to θ_{u2}, while the phase current will decrease after the switches are turned off when the BEMF is less than the DC link voltage.

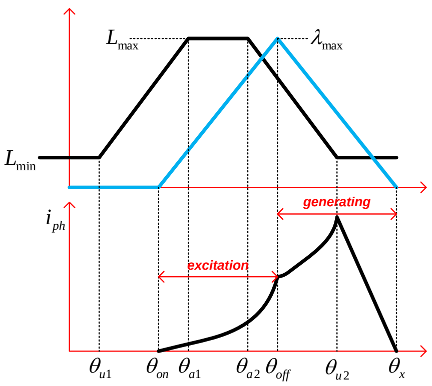

Figure 5. Profile of phase inductance, linked flux and current of SR machine

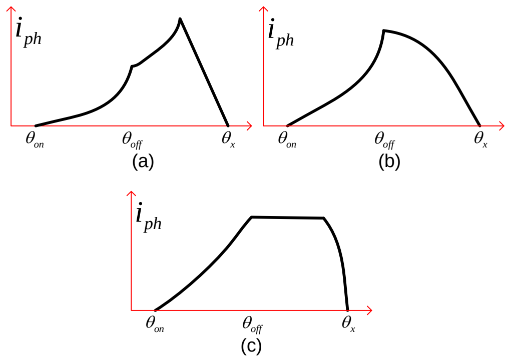

Figure 6. Phase current profiles of SR machine (a) BEMF>Vin (b) BEMF < Vin (c) BEMF = Vin

There are two control strategies for an SR machine operating in regenerative mode. In high speed operation, a single pulse based control strategy is implemented to excite the stator winding by selecting proper turn-on and turn-off angles. Meanwhile, in medium and low speed rotation, pulse width modulation based current controller is usually used, this controller will force the phase current to the desired level.

Under single pulse-based control strategy, during the excitation process, the power required to magnetize the stator winding (P_{exc}) can be expressed as (Ling, et.al., 2017).

$$P_{exc} = \int_{t_{on}}^{t_{off}} V_{in} i_{ph}(t)dt \quad \text{(Equation 5)}$$

where,

P_{exc} = power to magnetize the stator winding

Meanwhile during generating process, power which is generated by the stator winding (P_{gen}) and then it is sent back to the DC-link is expressed as

$$P_{gen} = \int_{t_{off}}^{t_x} V_{in} i_{ph}(t)dt \quad \text{(Equation 6)}$$

where,

P_{gen} = power which is generated by the stator winding

The output power of SR machine under regenerative mode (P_{out}) is determined by

$$P_{out} = P_{gen} - P_{exc} \quad \text{(Equation 7)}$$

where,

P_{out} = output power of the SRM under regenerative mode

2.2 Control Strategy in Regenerative Mode

The aim of the proposed control strategy is to achieve optimal regenerative mode operation based on single pulse excitation. This strategy will make the SR machine generate optimal output power to save more amount of energy in regenerative mode for EV and HEV. This strategy requires the understanding of the excitation angle impacts. Phase stator currents with three different turn-on angles and the same turn-off angles are shown in Fig.7. The turn-on angles are denoted as θ_1, θ_2 and θ_3 where $\theta_1<\theta_2<\theta_3$. The turn-on angle for the second case is set at aligned position, and then it can be expressed as

$$\theta_2 = \frac{\theta_{a1} - \theta_{a2}}{2} \qquad \text{(Equation 8)}$$

Where

θ_2 = the turn-on angle

θ_{a1} = the angle at which the rotor and stator poles begin to line up

θ_{a2} = the angle at which the rotor and stator alignment ends

For the phase stator windings are turned off at the same angle, the turn-on angle θ_1 will result in longer duration of excitation. At an instant angle θ_{off}, the peak of linked flux is higher than other cases of θ_2 or θ_3. With the higher linked flux, the higher BEMF can also be generated, and such a condition will result in the phase current which is sent back to DC-link increases in magnitude. Fig.8 can be used to investigate the comparison of each case. Fig.9 shows the DC-link current which has two part, namely the positive part and the negative part. The current with the largest negative side area indicates that the power sent to the DC-link will be greater. It can be seen, the case with turn-on angle equals to θ_1 results in the highest output power.

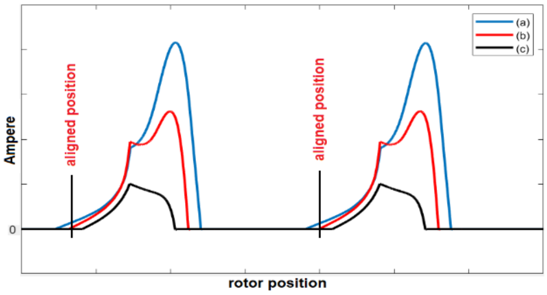

Figure 7. Comparison of phase currents for different turn-on angles (a) $\theta_{on} = \theta_1$ (b) $\theta_{on} = \theta_2$ (c) $\theta_{on} = \theta_3$

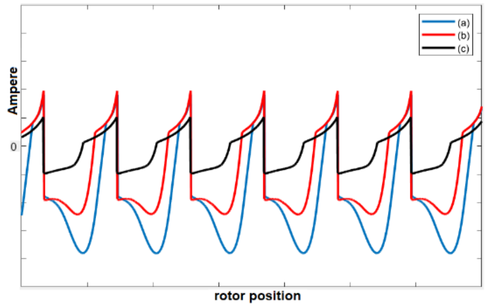

Figure 8. Comparison of DC-link currents for different turn-on angles (a) $\theta_{on} = \theta_1$ (b) $\theta_{on} = \theta_2$ (c) $\theta_{on} = \theta_3$

To find the phase stators inductance profiles, currents with small magnitude are injected into the stator windings. A curve which consists of phase stators inductance with respect to rotor position will be obtained. A three-phase SR machine is commonly embedded with three hall-effect sensors which are placed in 120 electric degrees one another.

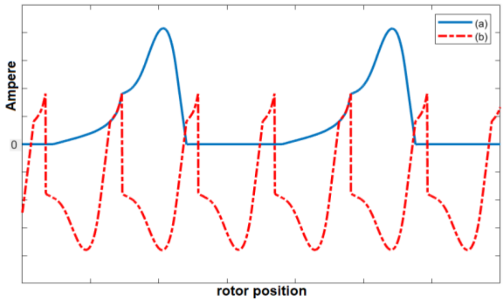

Figure 9. Under excitation angle θ1 (a) phase current (b) DC-link current

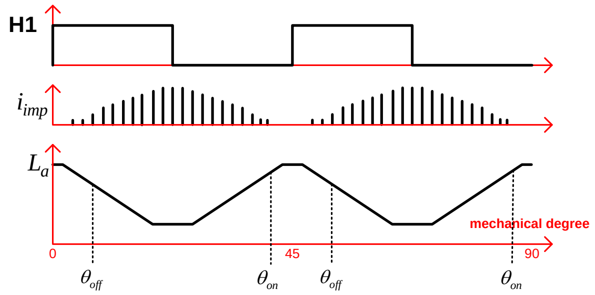

Figure 10. 12/8 SRM (a) one of hall-effect sensor signal (b) impulse current (c) inductance profile

When output signals of hall-effect sensors are directly used as the basis for commutation angles, the control strategy just has capability to generate certain angles. This is because in SR machine there are three Hall Effect sensors placed 120° apart from each other, so it is only able to give angle information in multiples of 60 electric degrees and it is impossible to select any value of angles to turn on and turn off the switches properly. By using input capture facility on 16-bit microcontroller dsPIC30F4012 as the core of the control system, proper commutations can be achieved. Steps of the proposed control strategy are depicted in Fig.11. When the IC (input capture) pin of the microcontroller is connected to the output signal of a Hall Effect sensor, content of the TIMER register will be captured on every rising edge of the input signal. The number of signals between two adjacent rising edge events constitutes the period of Hall Effect sensor (NPW). The instant number of pulses (NP) can also be performed which is started from 0 to NPW on every rising edge of hall-effect signal. The interrupt of the input capture process is used to force NP equals to 0 so the process will be restarted again.

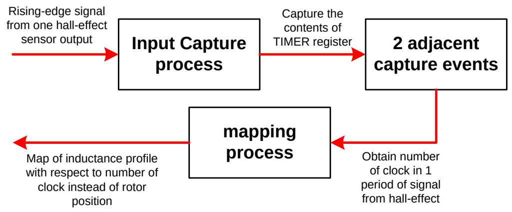

Figure 11. Steps of the proposed control strategy

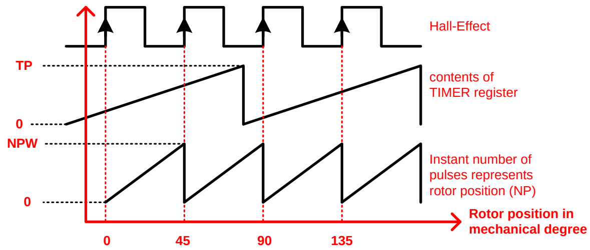

Figure 12. Relationship between hall-effect signal and instant number of pulses that represents rotor position (NP)

In the case of the 12/8 SR machine which is used in this research, the period of hall-effect signal is 45 mechanical degrees. Timing diagram of hall-effect signal and instant number of pulses which represents rotor position is shown in Fig.12. Finally, mapping of the phase inductance on the instant number of pulses which represents rotor position can be seen in Fig.13. Number of pulses where the stator winding starts (NP_{on}) and stops (NP_{off}) to be excited can be derived as

$$NP_{on} = \frac{\theta_{on}}{45} NPW \qquad \text{(Equation 9)}$$

where,

NP_{on} = number of pulses where the stator winding excitation starts

θ_{on} = the angle at which the excitation starts

$$NP_{off} = \frac{\theta_{off}}{45} NPW \qquad \text{(Equation 10)}$$

where,

NP_{off} = number of pulses where the stator winding excitation ends
θ_{off} = the angle at which the excitation ends

Turning on the stator winding of the SR machine for excitation under regenerative mode commonly takes place just before aligned position, it means that the stator winding has high inductance. Such a condition results in the phase current will increase and so the linkage flux. After the rotor becomes a temporary magnet, the excitation is turned off during the stator inductance profile is declining. This is based on the Faraday law, which states that BEMF will be generated when there is a change in magnetic flux. The generating current is then sent back to DC-link by opening the two switches. Some consideration must be chosen in order to have better efficiency. These are the width of excitation angle, machine parameters and minimizing the switching losses.

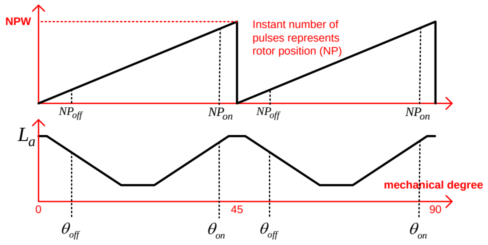

Figure 13. Mapping the phase inductance on the number of pulses that represents rotor position (NP)

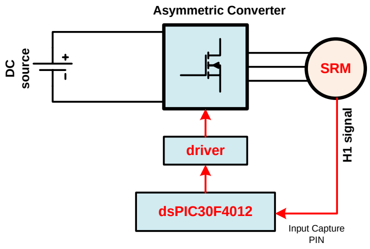

Figure 14. Scheme of the system using asymmetric converter

3. Results and Discussion

To support the analysis, experimental work was conducted by using the scheme shown in Fig.14 and the prototype shown in Fig.15. In the experimental work, a 12/8 switched reluctance machine with a three-phase asymmetrical topology was used as a power converter, and a 12 V battery was connected to the intermediate circuit. To operate this machine in a regenerative mode, the SR machine was coupled to a DC motor. A 16-bit microcontroller (dsPIC30F) was used as the core of the control strategy for it provides some features include input capture, high speed operation, low watt and external interrupt. To determine the phase inductance profiles, low voltage pulses were applied to the phase stator windings and the phase stator currents were measured. These are shown in Fig.16. It can be seen that each phase inductance profile is shifted by 120 electrical degrees. From these measurements, the inrush and outrush angles are determined. Using the input capture capabilities available on the dsPIC30F chip, any rotor positions with smooth angles can be selected for the correct excitation angles. The SR machine was rotated at 1800 rpm for the study at two different turn-on angles (2.5^{o} before and after the aligned position), but at the same turn-off angle of 11^{o} (mechanical degrees) after the aligned position. These angles were taken because these can give significant different results.

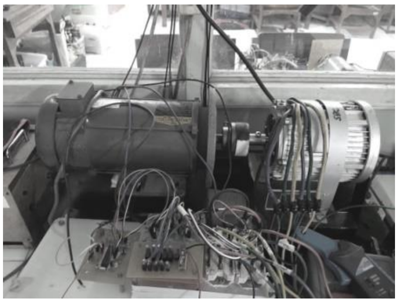

Figure 15. The prototype for experimental works

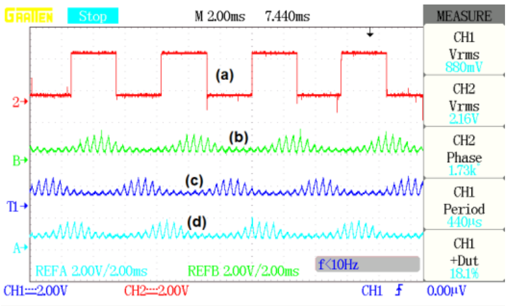

Figure 16. Experimental results under current impulse tests (a) hall-A (b) phase-A (c) phase-B (d) phase-C

Table 1. Components for the prototype

Items	Description

Machine type	Switched Reluctance
Stator / Rotor	12 poles / 8 poles
Digital Core	Microchip dsPIC30F4012
Switches	IGBT
Battery	12 V

The experimental results under the turn-on angle of 42.5° (or 2.5° before the aligned position is reached) are shown in Fig.17. When the excitation voltage is applied to the stator winding, the phase stator current will increase, and so will the associated flux. During the negative slope of the inductance profile when the excitation is turned off, the coupled flux with sufficient magnitude will result in the BEMF which is greater than the DC link voltage. Such a condition will cause the phase current to increase (based on Eq.3) and send greater amount of energy to the DC-link. Meanwhile, starting the excitation after the aligned position results in a lower value of the coupled flux at the end of the excitation, then the lower BEMF is also generated. When this BEMF is equal to the DC link voltage, the phase current will flow with almost constant value as shown in Fig.18. The output power of the SR machine operated as a generator can be compared with Fig.17a and Fig.18a. They show that the case under 42.5° turn-on angle contributes more power to the intermediate circuit. This is due to the intermediate circuit current with a larger area in negative polarity.

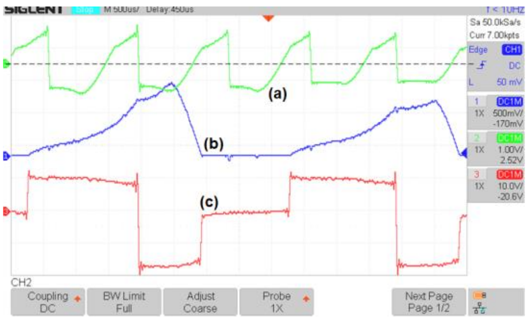

Figure 17. Results on 1800 RPM - excitation angle 42.5°-11°
(a) DC-link current (b) stator current (c) stator voltage

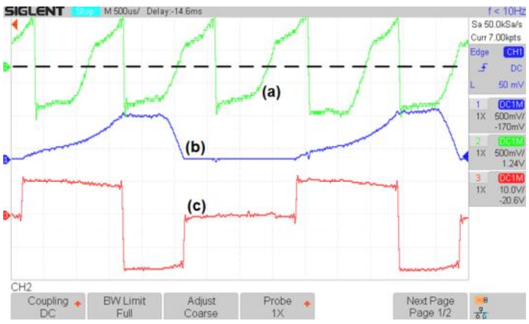

Figure 18. Results on 1800 RPM - excitation angle 2.5°-11°
(a) DC-link current (b) stator current (c) stator voltage

The magnitude of the BEMF is also influenced by the speed of the rotor of the SR machine. Experimental work was also carried out using the same excitation angles as in the previous work, but at a reduced speed. The rotor was rotated at 1200 rpm and then the phase currents were investigated. Under the excitation angle of 42.5°, reducing the speed will cause the BEMF to decrease. When this BEMF has the magnitude equal to the intermediate circuit voltage, the nearly constant current will flow in the phase stator (Fig.19). Reducing the speed from 1800 rpm to 1200 rpm under a switch-on angle of 2.5° will cause the phase current to decrease (Fig.20). By examining the intermediate circuit current, the effectiveness of energy saving during the regenerative operation of the SR machine can be checked. If the area of the negative polarity intermediate circuit current is larger than that of the positive polarity current, the energy saving can be achieved.

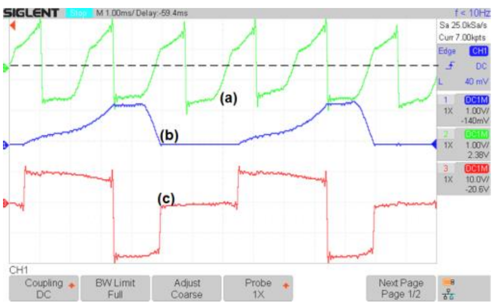

Figure 19. Results on 1200 RPM - excitation angle 42.5°-11°
(a) DC-link current (b) stator current (c) stator voltage

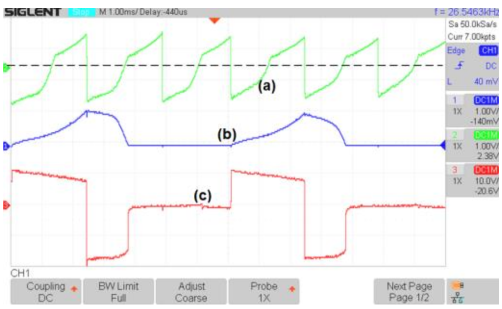

Figure 20. Results on 1200 RPM - excitation angle 2.5°-11°
(a) DC-link current (b) stator current (c) stator voltage

5. Conclusions

The analysis of a switched reluctance machine in regenerative mode has been described. The selection of the excitation angles determines the amount of power that is sent back to the DC bus. Turning on the excitation just before the aligned position between the stator and rotor results in the BEMF having a larger magnitude. If its magnitude is greater than the DC link voltage, the stator current will increase at the end of the excitation. Such conditions will increase the efficiency of the regenerative mode for more amount of energy can be saved. Due to Eq.7, this results in generating power greater than power for excitation. To obtain arbitrary angles with smooth values, the input capture function available in some microcontrollers can be implemented.

Acknowledgements

This work was supported by Directorate of Research and Community Service, Directorate General of Research Strengthening and Development, The Ministry of Research and Technology / National Council of Research and Innovation, Republic of Indonesia under the scheme of PTUPT 2021 and contract number 312/SP2H/LT/DRPM/2021.

References

Ai-de, X., He, K. and Cao, Y., 2016. Torque Ripple Reduction of SRM Using Optimized Voltage Vector in DTC. *2016 IEEE Vehicle Power and Propulsion Conference (VPPC)*.

Ai-de, X., Zang, W. and Ren, P., 2018. Comparison of Torque Ripple Reduction for Switched Reluctance Motor Based on DTC and DITC. *2018 13th IEEE Conference on Industrial Electronics and Applications (ICIEA)*.

Aiso, K. and Akatsu, K., 2020. High Speed SRM Using Vector Control for Electric Vehicle. *CES Transactions on Electrical Machines and Systems* , vol. 4(1), pp. 61-18.

Arifin, A., Al-Bahadly, I. H. and Mukhopadhyay, S. C., 2012. Simulation of Switched Reluctance Generator in Low and Medium Speed Operations for Wind Energy Application. *International Scholarly Research Network*, vol. 2012, pp. 1-13.

Bogusz, P., 2017. The novel control method of switched reluctance generator. *Archives of Electrical Engineering*, vol. 66(2), pp. 409-422.

Cheng, H., Wang, Z., Yang, S., Huang, J. and Ge, X., 2020. An Integrated SRM Powertrain Topology for Plug-In Hybrid Electric Vehicles With Multiple Driving and Onboard Charging Capabilitie. *IEEE Transactions on Transportation Electrification* , vol. 6(2), pp. 578 – 591.

Fernando, W. U. N., 2014. Control of Switched Reluctance Generators in Continuous Conduction Mode. *2014 IEEE Energy Conversion Congress and Exposition (ECCE)*.

Kurian, S. and Nisha, G. K., 2015. Torque Ripple Minimization of SRM Using Torque Sharing Function And Hysteresis Current Controller", *2015 International Conference on Control, Communication & Computing India (ICCC)*.

Li, H., Bilgin, B. and Emadi, A., 2019. An Improved Torque Sharing Function for Torque Ripple Reduction in Switched Reluctance Machines. *IEEE Transactions on Power Electronics* , vol. 34(2), pp. 1635 – 1644.

Ling, L., Dong, L. and Liao, X., 2017. Comparison of Two Control Methods of Switched Reluctance Generator. *2017 12th IEEE Conference on Industrial Electronics and Applications (ICIEA)*.

Oprasic, N., Masic, S. and Smaka, S., 2013. Excitation Parameters and Stability of Open Loop Operated Self-Excited Switched Reluctance Generator", *2013 International Electric Machines & Drives Conference*.

Peng, W., Gyselinck, J., Ahn, J. W. and Lee, D. H., 2018. Torque Sharing Function Control of Switched Reluctance Machines with Reduced Current Sensors. *CES Transaction on Electrical Machine and Systems* , vol. 2(4), pp. 355 – 362.

Sikder, C., Husain, I. and Sozer, Y., 2014. Switched Reluctance Generator Control for Optimal Power Generation With Current Regulation. *IEEE Transactions on Industry Applications*, vol. 50(1), pp. 307-316.

Sun, Q., Wu, J., Gan, C., Si, J., Guo, J. and Hu, Y., 2019. Cascaded Multiport Converter for SRM-Based Hybrid Electrical Vehicle Applications. *IEEE Transactions on Power Electronics*, vol. 34(12), pp. 11940 – 11951.

Tiwari, K. and Saxena, R., 2019. Speed Control of 8/6 Switched Reluctance Motor for Light Electric Vehicle. *2019 IEEE 5th International Conference for Convergence in Technology (I2CT)*.

Vujicic, V. P. and Calasan, M. P., 2016. Simple Sensorless Control for high-speed Operation of Switched Reluctance Generator", *IEEE Transactions on Energy Conversion*, vol.31(4), pp. 1325 – 1335.

Wahyu, G. D. and Riyadi, S., 2019. PWM Control Strategy of Regenerative Braking to Maximize The Charging Current into The Battery in SRM Drive", *2019 International Seminar on Application for Technology of Information and Communication (iSemantic)*, pp. 523-527.

Wang, W., Chen, H., Wang, Q., Dou, Y., Yan, S., Liu, Z., Huo, Y., Wang, Y., Wang, T. and He, D., 2017. Control system of switched reluctance generator. *2017 IEEE Conference of Russian Young Researchers in Electrical and Electronic Engineering (EIConRus)*.

Wei, Y., Qishuang, M., Poming, Z. and Yangyang, G., 2016. Torque Ripple Reduction in Switched Reluctance Motor Using a Novel Torque Sharing Function. *2016 IEEE/CSAA International Conference on Aircraft Utility Systems (AUS)*.

Yan, N., Cao, X. and Deng, Z., 2019. Direct Torque Control for Switched Reluctance Motor to Obtain High Torque-Ampere Ratio. *IEEE Transactions on Industrial Electronics*, vol. 66(7), pp. 5144 – 5152.

Zine, M., Labiod, C., Ikhlef, M., Srairi, K. and Benbouzid, M., 2023. Improving Efficiency and Power Output of Switched Reluctance Generators through Optimum Operating Parameters, *Machine* , vol.11, no.8, pp.1-19

Zhu, Y., Wu, H. and Zhang, J., 2020. Regenerative Braking Control Strategy for Electric Vehicles Based on Optimization of Switched Reluctance Generator Drive System", *IEEE Access*, vol. 8, pp. 76671-76682.